Original citation:
Jia, Ning, Sanchez Silva, Victor, Chang-Tsun, Li and Mansour, Hassan (2015) The influence of segmentation on individual gait recognition. In: 7th IEEE International Workshop on Information Forensics and Security (WIFS) 2015, Roma Tre University, Italy, 16-19 Nov 2015. Published in: 2015 IEEE International Workshop on Information Forensics and Security (WIFS), pp. 1-6.

Permanent WRAP url:
http://wrap.warwick.ac.uk/75550

http://wrap.warwick.ac.uk

The Influence of Segmentation On Individual Gait Recognition

Ning Jia, Victor Sanchez, Chang-Tsun Li
Department of Computer Science
University of Warwick
Coventry, UK
Email: n.jia@warwick.ac.uk
V.F.Sanchez-Silva@warwick.ac.uk
C-T.Li@warwick.ac.uk

Hassan Mansour
Mitsubishi Electric Research Laboratories,
Cambridge, USA
Email: mansour.hassan@gmail.com

Abstract—The quality of the extracted gait silhouettes can hinder the performance and practicability of gait recognition algorithms. In this paper, we analyse the influence of silhouette quality caused by segmentation disparities, and propose a feature fusion strategy to improve recognition accuracy. Specifically, we first generate a dataset containing gait silhouette with various qualities generated by different segmentation algorithms, based on the CASIA Dataset B. We then project data into an embedded subspace, and fuse gallery features of different quality levels. To this end, we propose a fusion strategy based on Least Square QR-decomposition method. We perform classification based on the Euclidean distance between fused gallery features and probe features. Evaluation results show that the proposed fusion strategy attains important improvements on recognition accuracy.

I. INTRODUCTION

Gait has drawn great attention over the past decade as a behavioural biometric modality that can be acquired at a distance in a non-invasive manner. Because of the great potential of this biometric trait in various fields such as remote surveillance and authentication, various algorithms have been recently proposed for person identification. These algorithms can be classified into two categories: model-based or appearance-based approaches. Model-based approaches rely on the extraction of parameters from the subjects' body and walking cycle to construct a structural model of human motion [1]. Appearance-based approaches, on the other hand, rely on spatio-temporal representations of gait, which may be directly obtained from the acquired gait sequences, such as binary gait silhouette. A detailed review of gait recognition algorithms, gait representations and databases may be found in the work by Makihara et al. [2].

Despite its many advantages, gait recognition is not as reliable as other biometric traits. Different factors such as age, clothes, walking surfaces, viewing angles, and health condition of the individuals may result in a poor recognition performance. Furthermore, recognition efficiency may be hindered if the associated gait gallery and probe silhouettes are acquired under different conditions. The quality of the silhouette can be influenced, for example, by the background environment when

capturing gait sequences and the accuracy of the segmentation method used to detect the gait silhouette.

Only a limited number of solutions reported in the literature have studied the effect of gait silhouette quality on the performance and practicability of model-free gait recognition algorithms. Sarkar et al. [3] discuss silhouette segmentation errors in the HumanID Gait Challenge Problem data set due to the shadow of the individuals, varying lighting conditions and moving objects in the background. In [4], Liu et al. observe that if gallery and probe gait sequences are captured under the same conditions, and are segmented by the same method, the recognition accuracy may be high even if the data quality is poor. Zhang et al. [5] and Yu et al. [6] address the issue of poor recognition accuracy when low-resolution gait silhouettes are used. In [7] Yu et al. propose a method to deal with extreme low frame-rate gait sequences using Random Subspace Method (RSM).

In this work, we study the case when quality differences exist between gallery and probe data, which are caused by applying different segmentation algorithms on gallery and probe video sequences to detect the corresponding gait silhouettes. We are particularly interested in the following two scenarios. 1) The gait data related to an individual to be recognized (i.e., the probe data) is not captured under ideal conditions, and therefore the associated gait silhouettes may be noisy and inaccurately segmented; whereas the stored gait data (gallery data) is captured in noise-free environments, or vice versa. 2) The silhouettes extracted from gallery and probe data are obtained using different segmentation algorithms, which may result in very different features[1].

Based on these scenarios, we propose a classier fusion strategy based on least square QR- decomposition (LSQR). Our approach uses GEIs [8], as it is one of the most popular and efficient methods to represent gait features. We first create a dataset by employing different segmentation algorithms on gait video sequences to generate silhouettes with segmentation

---

[1] A simple example is that a segmentation algorithm generates shadow-free gallery silhouettes, while another algorithm cannot generate shadow-free probe silhouettes. The shadow can then be considered as features (or noise) of the gallery silhouettes, thus affecting recognition accuracy.

disparities. The dataset is divided into training, gallery and probe sets, where the training set is for discriminant learning. We project gallery and probe data into a discriminant subspace to generate gallery and probe feature sets. The gallery features are fused using LSQR, thus generating more gallery representations, which are considered as classifiers to match with probe features. The output of all classifiers goes through a majority voting process, where the voting result represents the final classification decision. Local Fisher Discriminant Analysis (LFDA) is employed as the discriminant learning approach. Evaluation results show that our fusion strategy improves recognition accuracy compared to using only LFDA, or using a fusion strategy that assigns equal importance to all features.

The rest of the paper is organized as follows. Section 2 briefly reviews some background information, including the discriminant learning and majority voting method used in this work. Section 3 details the proposed approach as well as the dataset and experimental design. Section 4 presents the evaluation results and related discussions. Finally, Section 5 draws conclusions.

II. BACKGROUND INFORMATION

A. Gait Energy Image - GEI

Assume there are N gait silhouettes, represented as binary images, in one gait cycle. A GEI $G(x, y)$ is defined as $G(x, y) = \frac{1}{N} \sum_{k=1}^{N} I_k(x, y)$, where $I_k(x, y)$ is the kth binary image, and (x, y) denotes the pixel coordinates [8]. Examples of GEIs are shown in the rightmost column of Figure 2.

Consider n GEI samples that are stored as d-dimensional column vectors in a matrix $X = \{x_1, x_2, ..., x_n\}$, $x_i \in \Re^d$, $i \in \{1, 2, ..., n\}$. Let W be the transformation matrix that projects the original space onto an r-dimensional subspace, where $d \gg r$. The new feature matrix in the subspace is denoted as $Y = \{y_1, y_2, ..., y_n\}$, where $y_i \in \Re^r$. The transformation matrix for each element is given by $y_i = W^T x_i$, $i \in \{1, 2, ..., n\}$.

B. Dimensionality Reduction through PCA

Principle Component Analysis (PCA) is used as an approach to avoid singularities in further covariance matrix calculations [9] in LFDA. Following the notations above, the covariance matrix of the GEI matrix X is calculated as $S = \frac{1}{n} \sum_{i=1}^{n} (x_i - \mu)(x_i - \mu)^\top$, where μ is the sample mean, $\mu = \frac{1}{n} \sum x_i$, $i \in \{1, 2, ..., n\}$. The leading r vectors with corresponding r non-zero eigenvalues are computed and selected by the eigen-decomposition of the covariance matrix.

C. Discriminant Learning Using LFDA

Sugiyama [10] propose a novel subspace learning method called Local Fisher Discriminant Analysis (LFDA), which embeds within-class similarity matrices into local within-class scatter matrices and local between-class scatter matrices,

denoted as $\tilde{S}^{(w)}$ and $\tilde{S}^{(b)}$, respectively. These matrices are formulated as follows:

$$\tilde{S}^{(w)} = \frac{1}{2} \sum_{i,j=1}^{n} \tilde{W}_{i,j}^{(w)} (x_i - x_j)(x_i - x_j)^\top,$$
$$\tilde{S}^{(b)} = \frac{1}{2} \sum_{i,j=1}^{n} \tilde{W}_{i,j}^{(b)} (x_i - x_j)(x_i - x_j)^\top, \quad (1)$$

and

$$\tilde{W}_{i,j}^{(w)} = \begin{cases} 1/n_\ell & if\, y_i = y_j = \ell, \\ 0 & if\, y_i \neq y_j, \end{cases}$$
$$\tilde{W}_{i,j}^{(b)} = \begin{cases} 1/n - 1/n_\ell & if\, y_i = y_j = \ell, \\ 1/n & if\, y_i \neq y_j. \end{cases} \quad (2)$$

where n_ℓ is the number of samples in class ℓ, with $\sum_{\ell=1}^{c} n_\ell = n$. The transformation matrix of LFDA is then defined as:

$$W_{LFDA} = \arg\max_{W \in \Re^{d \times r}} \left[tr\left(\frac{W^\top \tilde{S}^{(w)} W}{W^\top \tilde{S}^{(b)} W}\right) \right]. \quad (3)$$

The transformation matrix W_{LFDA} is computed by solving the generalized eigenvalue problem of $\tilde{S}^{(w)}$ and $\tilde{S}^{(b)}$. LFDA has the ability to separate data from different classes while clustering data from the same class as close as possible, while keeping the neighbourhood structures within the same class.

D. Majority Voting

The majority voting method applied in this work is based on the max rule [11][12][13]. Let us assume that for individual x_i, there are p possible output labels computed by q classifiers, which are denoted by $l_k \in \{l_1, l_2, ..., l_p\}$. Let $n_{l_k} \leq q$ denote a score assigned to label l_k representing the number of classifiers who generated label l_k. Individual x_i is then assigned a label according to the following rule:

$$assign \quad x_i \to l_k, \quad if$$
$$n_{l_k} = max(n_i), \quad n_i = \{n_{l_1}, n_{l_2}, ..., n_{l_p}\}. \quad (4)$$

If $n_{l_i} = n_{l_j}$, $i, j \in \{1, 2, ..., p\}$, x_i is randomly assigned label l_i or l_j.

III. PROPOSED APPROACH

Fig. 1 shows the block diagram of the proposed approach. In the next subsections, we first describe the data used in our experiments, followed by a more detailed description of our approach.

A. Dataset Design

In order to build gait dataset containing silhouettes with different segmentation discrepancies, we combine background subtraction (BS), de-noising, and frame differentiation (FD), to generate different segmentation approaches. We also employ the Gaussian Mixture Model and Expectation Maximization (GMM & EM) segmentation method [3], and the Least Median of Squares (LMedS) segmentation method [14]. The segmented silhouettes obtained by each of these approaches is used to generate binary images (and GEIs) at a specific quality. The quality levels and the corresponding segmentation
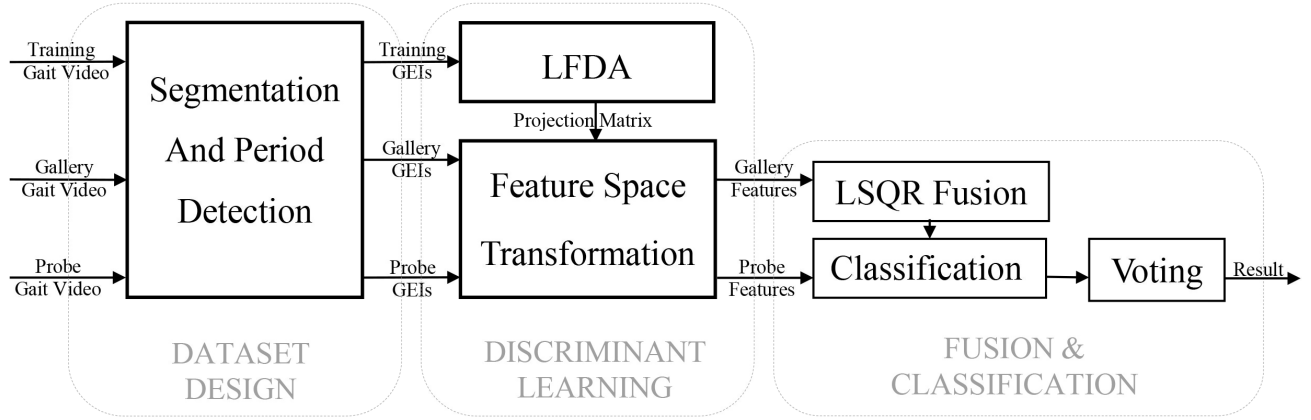
Fig. 1. Block Diagram of the proposed approach.

Quality	Segmentation Approach
Q.1	Approach 1: BS with Otsu's threshold
Q.2	Approach 2: Normalised BS plus dilation & erosion
Q.3	Approach 3: BS with small threshold (1/3 of Otsu's)
Q.4	Approach 4: FD plus dilation & erosion
Q.5	Approach 5: GMM & EM method
Q.6	Approach 6: LMedS method

Fig. 2. Samples of gait silhouette and corresponding GEIs with different qualities (Q.1 to Q.6) for the same subject. For each row, the first 11 images are the binary silhouettes obtained after segmentation. while the rightmost image is the corresponding GEI.

approaches used are listed in Table I. The segmentation approaches are explained in the following paragraphs.

Approach 1: A pixel is marked as foreground if $|I_t - B_t| > threshold$, where I_t refers to an image with both foreground and background objects and B_t contains only background objects. The threshold is set using Otsu's method[15].

Approach 2: The background image is normalized to eliminate the negative effects of noise. Thus $|I_t - avgB_t| > threshold$ where $avgB_t = B_t / \sum p_{i,j}$; $p_{i,j}$ refers to the value of pixel i, j in B_t. The threshold is set using Otsu's method. As the obtained foreground may comprise several disconnected regions, dilation and erosion operations are performed to generate the final foreground.

Approach 3: A small threshold is used in order to introduce a distinct contrast in the segmented silhouettes and to include more background objects in the foreground; namely $|I_t - B_t| > threshold/3$.

Approach 4: FD is used to mark the moving foreground pixels, $I_t - I_{t-1} > threshold$, where the threshold is set using Otsu's method. In addition, dilation and erosion operations are used in order to connect the disconnected regions comprising the foreground.

Approach 5: The GMM and EM method, as introduced in the baseline algorithm of Sarkar et al. [3].

Approach 6: The LMedS method, as is introduced in [14].

Using the distinct segmentation approaches tabulated in Table I, each gait sequence can generate six sequences with different segmentation discrepancies. For each of these six sequences, we compute the corresponding GEI. Figure 2 shows sample GEIs with the six different qualities.

B. Discriminant Learning

We select r of the total n eigenvectors generated by PCA, when the sum of the r corresponding eigenvalues are above 99% of the sum of all eigenvalues. LFDA is employed after reducing the dimensions of the training GEIs by using PCA. The generated transformation matrix W_{trans} is $W_{trans} = W_{LFDA}^\top W_{PCA}^\top$. We keep $(c-1)$ eigenvectors with r largest eigenvalues, where c denotes the number of classes in X.

C. Fusion and Classification

It is mentioned in [16] that an efficient way of combining classifiers is to put them into groups and apply a different fusion strategy to each group. An important factor to consider during grouping is the level of diversity of classifier types. However, it is hard to acquire prior knowledge of the optimal strategy for grouping classifiers and applying fusion strategies.

In this work, the gallery features with different segmentation discrepancies are fused in an exhaustive manner using a set of weights generated by LSQR, and each set of fused features is considered as one classifier. In other words, each distinct classifier is created by fusing gallery features with three different qualities. With 6 qualities in total, the number of generated fusion classifiers is $N_c = 6!/((6-3)! * 3!) = 20$. A set of weights are assigned to the three gallery features to be fused. For example, if a classifier comprises gallery features at qualities Q.1, Q.2 and Q.3, the features are fused as $g_f = w_1 * g_{Q.1} + w_2 * g_{Q.2} + w_3 * g_{Q.3}$, where $w_i, i \in \{1, 2, 3\}$ are the corresponding weights for the gallery features. The values of weights w_i are calculated as a vector by:

$$w = \arg\min_{w} \|gallery * w^\top - probe\|, \qquad (5)$$

where $gallery$ and $probe$ are column vectors containing the gallery data at different qualities to be fused, and the corresponding probe data, respectively

Let us denote the set of gallery GEI vectors by $\mathbf{g}$, and the set of probe GEI vectors by $\mathbf{p}$. Following the subspace transformation processes in Section III-B, the gallery feature sets $\{\hat{\mathbf{g}}\}$ and probe feature sets $\{\hat{\mathbf{p}}\}$ are obtained as follows:

$$\begin{aligned}
\{\hat{\mathbf{g}}\} : \hat{g}_i = W_{trans}G_i, \ i \in \{1, 2, ..., n_1\} \\
\{\hat{\mathbf{p}}\} : \hat{p}_j = W_{trans}P_j, \ j \in \{1, 2, ..., n_2\}
\end{aligned} \qquad (6)$$

where n_1, n_2 are the total number of GEIs in gallery and probe data sets, respectively; and G_i, and P_i denote the GEI representations of gallery and probe data, respectively. The centroid of class l in $\{\hat{\mathbf{g}}\}$ is calculated as $mg_l = \frac{1}{n_l}\sum_{\hat{\mathbf{g}} \in \hat{g}_l} \hat{\mathbf{g}}$, where $\hat{g}_l$ is the set of gallery feature vectors in class l. The centroid of class l in $\{\hat{\mathbf{p}}\}$ is calculated in the same way and is denoted as mp_l. The classifier is then defined as:

$$D(mg_l, mp_i) = \|mp_i - mg_l\|, i = 1, 2, ...c. \qquad (7)$$

If $D(mg_l, mp_l) = \min_{i=1}^{c} D(mg_l, mp_i)$, the probe feature vector is assigned to the right class label l. The classification results of all classifiers used in our fusion strategy go through the majority voting process to obtain the final recognition result.

IV. EXPERIMENT AND RESULT

We use the gait sequences of CASIA Dataset B to generate GEIs with 6 different qualities, as previously described. CASIA Dataset B comprises video sequences for 124 individuals. We use the video sequences of first 62 individuals as the training data. The sequences of the remaining 62 individuals are used as gallery and probe data. The frame size of all sequences is 320×240, and the frame rate is 25 fps. All 6 segmentation approaches produce binary silhouettes with a size of 128×88. As this work aims at studying the effect of gait silhouette quality on recognition, other factors that may influence the recognition performance are excluded. Therefore, only normal gait sequences are chosen from CASIA Dataset B, without the factors of carrying objects, different clothes, or different view angles.

TABLE II
RECOGNITION RATES (%) WITHOUT DISCRIMINANT LEARNING AND FUSION BETWEEN GALLERY (G) AND PROBE (P) WITH DIFFERENT QUALITIES. PERCENTAGES IN BOLD INDICATE THE HIGHEST RECOGNITION RATE.

G \ P	Q.1	Q.2	Q.3	Q.4	Q.5	Q.6
Q.1	**85**	12	7	10	80	70
Q.2	12	**67**	17	8	10	35
Q.3	17	15	**78**	5	17	8
Q.4	15	8	5	**38**	18	15
Q.5	83	12	7	13	**83**	63
Q.6	58	25	5	10	43	**97**

A. Evaluation Without Subspace Learning

We first evaluate the recognition rates without discriminant learning and fusion. The recognition rates, in percentage, are shown in Table II. Two observations can be drawn from this table:

1) The entries in the main diagonal represent the matching results between gallery and probe data with the same quality. These values are generally the highest values among each column, suggesting that when both gallery and probe data have same quality, the best matching results are attained. However, matching across gallery and probe with different qualities obtains low results in most cases, with some exceptions; for example the matching rates between Q.1 and Q.5. This indicates that different segmentation approaches might generate silhouettes with similar quality.

2) The entries outside the main diagonal show that the quality disparity between gallery and probe data indeed decreases the recognition accuracy. In some cases, the matching rate between data segmented using the same approach can still be very low, which indicates that the segmentation approach may be inappropriate for the sequences (see for example Q.4 gallery matched with Q.4 probe).

B. Evaluation With Discriminant Learning

We measure the similarity between gallery and probe features generated by subspace transformation. The recognition rates are shown in Table III. Note that by using dimensionality reduction plus LFDA, the figures in Table III significantly improve compare with the figures in Table II.

C. Fusion Between Qualities with Majority voting

Finally, we evaluate the recognition rates attained by using our fusion approach with majority voting. In this evaluation, we are also interested in considering the case when data contained in the probe set with a specific quality is not present in the gallery data. This attempts to represent the situation where the quality of the probe data is different from that of the gallery data. Recognition rates are tabulated in Table IV. The notation for this table are as follows:

TABLE III
RECOGNITION RATES (%) USING LFDA BETWEEN GALLERY (G) AND
PROBE (P) WITH DIFFERENT QUALITIES. PERCENTAGES IN BOLD
INDICATE THE HIGHEST RECOGNITION RATE.

G \ P	Q.1	Q.2	Q.3	Q.4	Q.5	Q.6
Q.1	**95**	75	63.3	20	93.3	95
Q.2	85	**85**	83.3	30	78.3	91.7
Q.3	68.3	75	**95**	33.3	66.7	81.7
Q.4	48.3	46.7	70	**61.7**	56.7	68.3
Q.5	95	75	56.7	21.7	**95**	96.7
Q.6	88.3	66.7	65	23.3	85	**100**

TABLE IV
THE RECOGNITION RATES IN PERCENTAGE (%) FOR PROBE DATA WITH 6
SEs. DL(A): AVERAGE RATES OF LFDA; DL(H): HIGHEST RATES OF
LFDA; FDL(S): FUSION+LFDA USING SPLIT-EQUAL WEIGHT; FDL:
PROPOSED APPROACH; FDL(I): DEALING WITH INCOMPLETE GALLERY
DATA USING PROPOSED APPROACH

| Alg. | Probe | | | | | | |
	Q.1	Q.2	Q.3	Q.4	Q.5	Q.6	Avg.
DL-A	80	70.6	72.2	31.7	76.3	87	**68.3**
DL-H	95	85	95	61.7	95	100	**88.6**
FDL-S	90	78.3	83.3	33.3	88.3	96.7	**78.3**
FDL	95	85	90	58.3	95	98.3	**86.9**
FDL-I	95	76.7	73.3	23.3	93.3	95	**76.1**

- DL- A: LFDA. Average recognition rates for each column in Table III.
- DL-H: highest recognition rate in each column of Table III.
- FDL-S: LDFA plus fusion and majority voting. The weights are equal for the three gallery features to be fused, i.e., $w =$[1/3 1/3 1/3].
- FDL: LDFA plus fusion and majority voting, i.e. the proposed approach.
- FDL-I: the proposed approach with incomplete fusion, i.e., a particular quality contained in the probe data is not present in the gallery data.

The improvement of the fusion approach is evident compared to the recognition performance using a single classifier. The fusion strategy using LSQR attains higher recognition rates than the case of using equal weights (FDL-S). Note that results corresponding to FDL are similar to those corresponding to DL-H. This is expected, as the fusion strategy is capable of obtaining weights that results in the highest recognition rates when the quality of the probe data is in the gallery data during fusion. When the probe quality is not present in the gallery data, the recognition results are still high (see FDL-I).

D. Discussions

Experiment results suggests that the quality of the extracted binary silhouette images is particularly important for model-free gait recognition algorithms to perform accurately, since the segmentation errors might negatively affect the recognition rates. In [4], it is mentioned that a low gait silhouette quality may provide powerful features for gait recognition when both gallery and probe data have the same low quality. However, through our analysis, an inaccurate segmentation could lead to very low recognition rate, even when employing discriminant learning methods, see for example results for probe data with Q.4 in Table III.

One main shortcoming of LFDA, as in any other discriminant learning method, is that subjects represented by very low quality silhouettes cannot be recognized accurately. Nevertheless, if the quality of gallery and probe data are acceptable, even if they are very different, our fusion approach can improve the matching performance to a promising level.

V. CONCLUSION

This paper studied the performance of GEI-based gait recognition algorithms when a disparity in quality between gallery and probe data exists. To this end, we generated gait silhouettes with different segmentation discrepancies in order to represent different levels of data qualities.

A classifier fusion strategy in conjunction with discriminant learning was proposed to tackle the negative impact of quality disparity on matching rate. Specially, we proposed to generate weights by using LSQR to fuse gallery features and generate several classifiers. We then proposed to use majority voting to compute the final classification result. Experimental results on the CASIA Dataset B suggested that this approach provides better performance than the case of using a single classifier and the case of employing fusion with equal weights.

REFERENCES

[1] C. Wang, J. Zhang, L. Wang, J. Pu, and X. Yuan, "Human identification using temporal information preserving gait template," *Pattern Analysis and Machine Intelligence, IEEE Transactions on*, vol. 34, no. 11, pp. 2164–2176, Nov 2012.

[2] Y. Makihara, D. Matovski, M. S. Nixon, J. N. Carter, and Y. Yagi, "Gait recognition: Databases, representations, and applications," 2015.

[3] S. Sarkar, P. Phillips, Z. Liu, I. Vega, P. Grother, and K. Bowyer, "The humanid gait challenge problem: data sets, performance, and analysis," *Pattern Analysis and Machine Intelligence, IEEE Transactions on*, vol. 27, no. 2, pp. 162–177, Feb 2005.

[4] Z. Liu and S. Sarkar, "Effect of silhouette quality on hard problems in gait recognition," *Systems, Man, and Cybernetics, Part B: Cybernetics, IEEE Transactions on*, vol. 35, no. 2, pp. 170–183, April 2005.

[5] J. Zhang, J. Pu, C. Chen, and R. Fleischer., "Low-resolution gait recognition," *Systems, Man, and Cybernetics, Part B: Cybernetics, IEEE Transactions on*, vol. 40, no. 4, pp. 986–996, Aug 2010.

[6] Y. Guan, Y. Sun, C.-T. Li, and M. Tistarelli, "Human gait identification from extremely low-quality videos: an enhanced classifier ensemble method," *Biometrics, IET*, vol. 3, no. 2, pp. 84–93, June 2014.

[7] Y. Guan, C.-T. Li, and S. Choudhury, "Robust gait recognition from extremely low frame-rate videos," pp. 1–4, April 2013.

[8] J. Han and B. Bhanu, "Individual recognition using gait energy image," *Pattern Analysis and Machine Intelligence, IEEE Transactions on*, vol. 28, no. 2, pp. 316–322, Feb 2006.

[9] A. Webb and K. Copsey., *Statistical Pattern Recognition*, 3rd ed. Chichester: Wiley, 2011.

[10] M. S., "Dimensionality reduction of multimodal labeled data by local fisher discriminant analysis," *The Journal of Machine Learning Research*, vol. 8, pp. 1027–1061, 2007.

[11] Y. Guan, C. Li, and F. Roli, "On reducing the effect of covariate factors in gait recognition: a classifier ensemble method," *Pattern Analysis and Machine Intelligence, IEEE Transactions on*, vol. PP, no. 99, pp. 1–1, 2015.

[12] L. Kuncheva, J. Bezdek, and R. Duin, "Decision templates for multiple classifier fusion: an experimental comparison," *Pattern recognition*, vol. 34, no. 2, pp. 299–314, 2001.

[13] G. Veres, M. Nixon, L. Middleton, and J. Carter, "Fusion of dynamic and static features for gait recognition over time," in *Information Fusion, 2005 8th International Conference on*, vol. 2. IEEE, 2005, pp. 7–pp.

[14] L. Wang, T. Tan, H. Ning, and W. Hu, "Silhouette analysis-based gait recognition for human identification," *Pattern Analysis and Machine Intelligence, IEEE Transactions on*, vol. 25, no. 12, pp. 1505–1518, Dec 2003.

[15] M. Sezgin and B. Sankur, "Survey over image thresholding techniques and quantitative performance evaluation," *Journal of Electronic Imaging*, vol. 13, no. 1, pp. 146–168, 2004. [Online]. Available: http://dx.doi.org/10.1117/1.1631315

[16] D. Ruta and B. Gabrys, "An overview of classifier fusion methods," *Computing and Information systems*, vol. 7, no. 1, pp. 1–10, 2000.